Supplemental Data

C. elegans Anaplastic Lymphoma Kinase Ortholog SCD-2 Controls Dauer Formation by Modulating TGF-β Signaling

David J. Reiner, Michael Ailion, James H. Thomas, and Barbara J. Meyer

Supplemental Results

Mutant *che-1* Disruption of the ASE Sensory Neurons Suppresses TGF-β Daf-c Mutations

We genetically disrupted the function of the bilateral pair of ASE sensory neurons using *che-1* mutations. *che-1* encodes a transcription factor expressed primarily in ASE neurons. Mutations in *che-1* specifically disrupt all known sensory functions of the ASE neurons but not those of other sensory neurons [1], and expression of all known ASE-specific markers is abolished in *che-1* mutants [2]. Together, these observations indicate that *che-1* is necessary for proper ASE cell fate and function.

We constructed *che-1*; *daf-7(e1372)* double mutants using four different *che-1* alleles and found slight suppression of the *daf-7* Daf-c phenotype (Supplemental Table S2). Since weaker *scd-2* branch mutations, like *scd-2(sa303)* or *soc-1* alleles, only poorly suppressed the strong *daf-7(e1372)* Daf-c phenotype, we tested *che-1* suppression of *daf-14(m77)*, which is partially redundant with *daf-8* and therefore causes a weaker Daf-c phenotype [3]. *daf-8(e1393)* was not used in this analysis because it is closely linked to *che-1*. We found that *che-1* suppressed the Daf-c phenotype of *daf-14* at 25˚C, though to a lesser degree than *scd-2(ok565)*. We also assayed the response to exogenous dauer pheromone, and found these four mutants to be defective (Supplemental Table S2). Finally, a mutation in *che-1* weakly restored *cuIs5* GFP expression in a *daf-7* background, to a level comparable to that of a *soc-1* mutation. These data suggest that the ASE sensory neurons function in the dauer decision. Our observations are also consistent with the idea that HEN-1 is secreted from ASE and signals through the SCD-2 branch to modulate TGF-β signaling.

hen-1 is primarily expressed in ASE and AIY [4]. The fact that *che-1* mutants have a weaker dauer phenotype than *hen-1* or *scd-2* suggests that there may be other sources of HEN-1 in addition to ASE. To test this idea, we built a *che-1*; *daf-14; ttx-3* triple mutant in which ASE (*che-1)* and AIY(*ttx-3)* function is disrupted. The *che-1(p679)*; *daf-14(m77)*; *ttx-3(ot22)* triple mutant is comparable to *daf-14*; *ttx-3* and weaker than *daf-14; scd-2*, suggesting that the *che-1*; *ttx-3* mutant combination does not phenocopy *hen-1* or *scd-2* effects on dauer formation. This indicates that either there are other sources of HEN-1 in addition to ASE and AIY or that the *che-1* and *ttx-3* mutations do not fully disrupt HEN-1 secretion from these cells.

Supplemental Experimental Procedures

C. elegans Culturing and Genetics

Handling, maintenance and nomenclature of *C. elegans* strains were as described [5, 6]. Strains were derived from the wild-type strain N2, except *scd-2(sa935)*, which was derived from the wild isolate CB4507 [7, 8]. Animals were cultured on the *E. coli* strain TJ2, a derivative of OP50 [9].

Daf-c and Daf-d double and triple mutant combinations were constructed and confirmed as previously described [10]. Double mutant strains were constructed with *scd-2(y386)* and mutations in *let-23*, *sma-6*, *vab-1*, *vab-2*, *cam-1*, *daf-2*, *daf-1*, *daf-4*, *daf-7*, *ina-1*, *pat-3*, *mab-26*, *unc-5*, *unc-6*, *sax-3*, *mab-19* and *egl-15*, all of which encode receptors or ligands. The only interactions found were with dauer TGF-β signaling components.

For dauer assays, parents laid eggs at 22°C for 2-6 hours, and dauers were counted after 48 and 65 hours for 25ºC and 20ºC, respectively, except for *soc-1* and *sma-5* 25°C counts at 72 or 120 hours, respectively. Each assay was repeated multiple times, but the data in each figure panel are from strains assayed in parallel at the same time and do not represent pooling of data from multiple assays. Dauer pheromone assays used semi-purified pheromone prepared from worm extracts [11] and were performed as described [9].

scd-2(y386) was obtained from a 920,000 haploid genome deletion library screened by PCR [12]. *y386* was outcrossed 10 times to the *snb-1(md247)* balancer.

Mutations and Transgenes

LGI: *daf-8(e1393)*, *che-1(p679)*, *che-1(ot66)*, *che-1(ot27)*, *che-1(p692)*, *che-1(e1034)*, *mek-2(n2678)*, *hT2(I;III)*, *sup-11(n403)*, *dpy-5(e61)*, *smg-1(cc546*ts*)*, *scd-3(sa253)*.

LGII: *cog-1(ot28)*, *ptp-2(op194)*, *ptp-3(op147)*, *clr-1(e1745*ts*)*, *unc-4(e120)*, *daf-5(e1386)*, *mIn1mIs14* , *let-23(n1045)*, *unc-52(e1421)*, *sma-6(e1482)*, *vab-1(e2)*, *cam-1(gm122)*, *tra-2(q276)*, *ras-1(gk237)*, *ras-1(gk243)*.

LGIII: *daf-2(e1370)*, *daf-7(e1372)*, *daf-4(m63)*, *eT1(III;V)*, *hT2(III;I)*, *ina-1(gm39)*, *ina-1(gm144)*, *unc-32(e189)*, *mpk-1(ku1)*, *mpk-1(oz140)*, *mpk-1(n2521)*, *dpy-17(e164)*, *unc-79(e1068)*, *pat-3(ay84)*, *dpy-18(e364)*.

LGIV: *let-60(n2021*lf*)*, *let-60(n1046*gf*)*, *let-60(ga89*gf*)*, *let-60(ay75*gf*)*, *lin-45(*sy*96)*, *daf-1(n690)*, *unc-129(ev554)*, *vab-2(e96)*, *efn-4(bx80)*, *unc-5(e53)*, *jcIs1[ajm-1::gfp + pRF4(rol-6(*d*))]*, *cuIs2[C183::gfp + pRF4(rol-6(*d*))]*, *cuIs5[C183::gfp + pRF4(rol-6(*d*))]*.

LGV: *lsy-6(ot71)*, *let-472(s1605)*, *let-410(s815)*, *let-469(s1582)*, *unc-60(e677)*, *unc-46(e177)*, *dpy-11(e224)*, *unc-42(e270)*, *unc-68(e540)*, *unc-70(e524*gf*)*, *unc-*

*70(n493*gf*)*, *unc-70(n493n1171)*, *unc-76(e911)*, *scd-2(sa249)*, *scd-2(sa303)*, *scd-2(sa935)*, *scd-2(y386)*, *scd-2(ok565)*, *snb-1(md247)*, *daf-11(m47)*, *soc-1(n1789)*, *soc-1(n1788)*, *daf-28(sa191*gf*)*, *scd-4(sa321)*, *eT1(V;III)*, *sDf20*; *sDf30*, *unc-62(e644)*.

LGX: *ceh-36(ky640)*, *hen-1(ut236)*, *hen-1(tm501)*, *lin-15(n765*ts*)*, *daf-3(e1376)*, *daf-3(mgDf90)*, *sma-5(n678)*, *sli-1(sy143)*, *unc-1(e580)*, *daf-12(m20)*, *sax-3(ky123)*, *unc-6(ev400)*, *mab-19(bx38)*, *dpy-8(e130)*, *unc-6(e78)*, *egl-15(n484)*, *sem-5(n2030)*, *sem-5(n2019)*, *unc-10(e102)*, *xol-1(y9)*, *dpy-6(e14)*, *scd-1(sa248)*, *gmIs18[Pceh-23::gfp + pRF4(rol-6*(d))*]*.

Unknown map position: *edIs6[unc-119::gfp + pRF4(rol-6(*d*))*].

Extrachromosomal arrays: *yEx449[pDJR22(Pscd-2::gfp + pRF4(rol-6(*d*))]*, *yEx663[pDJR29.3(Plet-858::5'RNAi) + pPD118.33(myo-2::GFP)]*, *yEx667 [pDJR30.3(Pdaf-4::scd-2(neu*)) + pRF4(rol-6(*d*))]*, *yEx670[pDJR31.4(Plet-858::scd-2S) + pPD118.33(myo-2::GFP)]*, *saEx472[pTJ1369 + pBLH98(lin-15(+)]*.

Genetic Mapping and Complementation Tests

We found a modifier of GFP levels in the background of the original *cuIs2* strain. Outcrossed strains (4 times) without modifiers were used for subsequent *cuIs2* and *cuIs5* strain constructions and assays. We also found a modifier of *cuIs* strain GFP expression in the background of *let-60(n1046*gf*)*. After the modifier was removed by outcrossing, *let-60(n1046*gf*)* was found to have no effect on GFP reporter expression, nor did two other *let-60* gain-of-function alleles, *ay75* and *ga89*.

scd-2 was previously mapped to the region of *dpy-11* on LGV [8]. We mapped *scd-2* by its pheromone resistant phenotype. Three-factor mapping showed that *scd-2* lay close to the right of *dpy-11*. *scd-2* recombinant data were *dpy-11* (1/18) *scd-2* (17/18) *unc-76*, *dpy-11* (2/16) *scd-2* (14/16) *unc-42*, *dpy-11* (4/9) *scd-2* (5/9) *unc-70(*gf*)*, *dpy-11* (10/26) *scd-2* (16/26) *unc-70(*lf*)*, placing *scd-2* at approximately 40% of the distance between *dpy-11* and *unc-70*.

We also tested whether *sa321*, a previously identified Scd allele that mapped to LGV [8], was an allele of *scd-2*. *sa321* also confers slightly short body morphology, a mild egg-laying defect (Egl), male tail abnormalities (Mab), and resistance to dauer pheromone (data not shown). Of these pleiotropic defects, only the Scd and pheromone resistance phenotypes are shared with the five known *scd-2* alleles. *sa321* complemented *scd-2(sa935)* for the pheromone response phenotype and *scd-2(y386)* for the suppression of the *daf-7* Daf-c phenotype. We mapped *sa321* by its *daf-7* suppression phenotype to the *unc-62 dpy-11* interval (*unc-62* (4/10) *sa321* (6/10) *dpy-11*), which excludes *scd-2*. Therefore, *sa321* is not allelic with *scd-2*.

Because *soc-1* has a mild Scd phenotype and also maps to the *unc-62 dpy-11* interval, we tested *sa321* and *soc-1(n1789)* complementation. *sa321* and *soc-1* complement for the suppressor of *clr-1* and suppressor of *daf-7* phenotypes, and *sa321* fails to suppress the temperature-sensitive lethality of *clr-1*. Furthermore, *sa321* does not show the scrawny phenotype characteristic of the Soc mutations. We propose that *sa321* is an allele of a new Scd gene, which we name *scd-4*.

Dauer Formation

We encountered an unexpected phenomenon with dauer assays at UC Berkeley. In all dauer assays performed at Berkeley, between 20 and 60% of the dauers were actually partial dauers rather than full dauers. By DIC microscopy the partial dauers were of the described *daf-16* type [10]. This was true for all strains that formed dauers, regardless of the genotype. The same phenomenon was observed in multiple incubators from multiple manufacturers at different temperatures, and even incubators in different buildings. We tested strains, media, and bacterial food sources by swapping all three between the UW Seattle and UC Berkeley labs. Using Berkeley strains, media, and food, normal dauers were formed in Seattle, and using Seattle strains, media and food, a fraction of partial dauers were formed in Berkeley. We cannot explain this phenomenon, except to invoke an ambient effect on dauer formation in Berkeley. We discovered that when using the 25°C incubator in the Kenyon lab at UCSF, 100% normal dauers were formed, so we duplicated the assays shown here in that incubator, and found that the genetic relationships held true. Additional assays with *hen-1* and *che-1* were performed in the Goldstein lab at UNC, and 100% normal dauers were formed. We conclude that while we do not understand the cause of the phenomenon, it does not affect the genetic pathway interactions we are studying.

Molecular Cloning, Subcloning, and Transgenic Line Construction

scd-2(sa935); *lin-15(n765*ts*)* animals were injected with candidate cosmids and subclones at 10 ng/μl and pBLH98 *lin-15(+)* as the transformation marker at 60 to 90 ng/ml [13, 14], and array-bearing transformants were scored for rescue of the pheromone response phenotype (Figure 3).

All subclone joins and coding sequences subjected to PCR were sequenced. pDJR30.3 contains a 3.5 kb *daf-4* promoter, the complete *scd-2* cDNA with *neu** TM domain rather than the native SCD-2 TM, and the *unc-54* 3'UTR.

Transgenic lines [14] for non-rescue experiments used pPD118.33 *myo-2::gfp* at 25 ng/ml, resulting in strong GFP expression in the pharynx. pDJR30.3 (P_{daf-4}::*scd-2(neu*)*) was injected at 175 ng/μl (100% L1 arrest) and 50 ng/μl (much L1 arrest, but the representative transgene *yEx667* was isolated). For each construct a promoter-only construct was injected at the same concentration with the same co-injection markers and was found to cause no phenotype.

The sequence in the NCBI database mistakenly added a base (F44C4 bp 29544) to the false intron in exon 13 that would change the reading frame and lead to a stop codon if this intron were translated. All *scd-2* mutations were sequenced on both strands from at least two independent PCR products.

Splicing to the native intron 2 splice acceptor was eliminated in *sa303*, but the reading frame, and hence some receptor tyrosine kinase-encoding ability, were restored in some mRNA species by two mechanisms: splicing to a cryptic splice acceptor site in exon 3 and splicing to the native splice acceptor of intron 3 (data not shown).

Microscopy, 4D Videomicroscopy and Pharyngeal GFP Scoring

GFP photomicrographs were captured on a Zeiss Axioplan with a cooled 3-chip color digital video camera (Optronics, Leica Model LEI-750TD). Differential interference contrast (DIC) images were captured on Zeiss Axioplan (above) and Axioplan 2 microscopes with a Hamamatsu ORCA digital camera (Model C4742-95) and OpenLab software.

GFP expression in late L4 *cuIs2* and *cuIs5* bearing animals was visualized on the Zeiss Axioplan II scope. *cuIs2* and *cuIs5* GFP expression levels were very consistent within a specific genotype. We established baseline activities, whereby "+++++" represents the intensity of *cuIs2* or *cuIs5* alone (the two were indistinguishable), "+" represents the intensity of *daf-7*; *cuIs2/5*, and "+++" represents the intensity of *daf-8*; *cuIs2/5*, which was halfway between the two outliers in intensity. Then, all other genotypes were compared directly to these standards to assess their intensity. Many genotypes were the same intensity as one of these standards, but some were clearly of intermediate intensity, so a 5-point scale of intensity was established. In each case, greater than 90% of the animals of a given genotype could be unambiguously assigned to the same intensity category. A minimum of 20 GFP-expressing animals were scored blindly for each genotype to avoid scorer bias.

Supplemental Figure S1

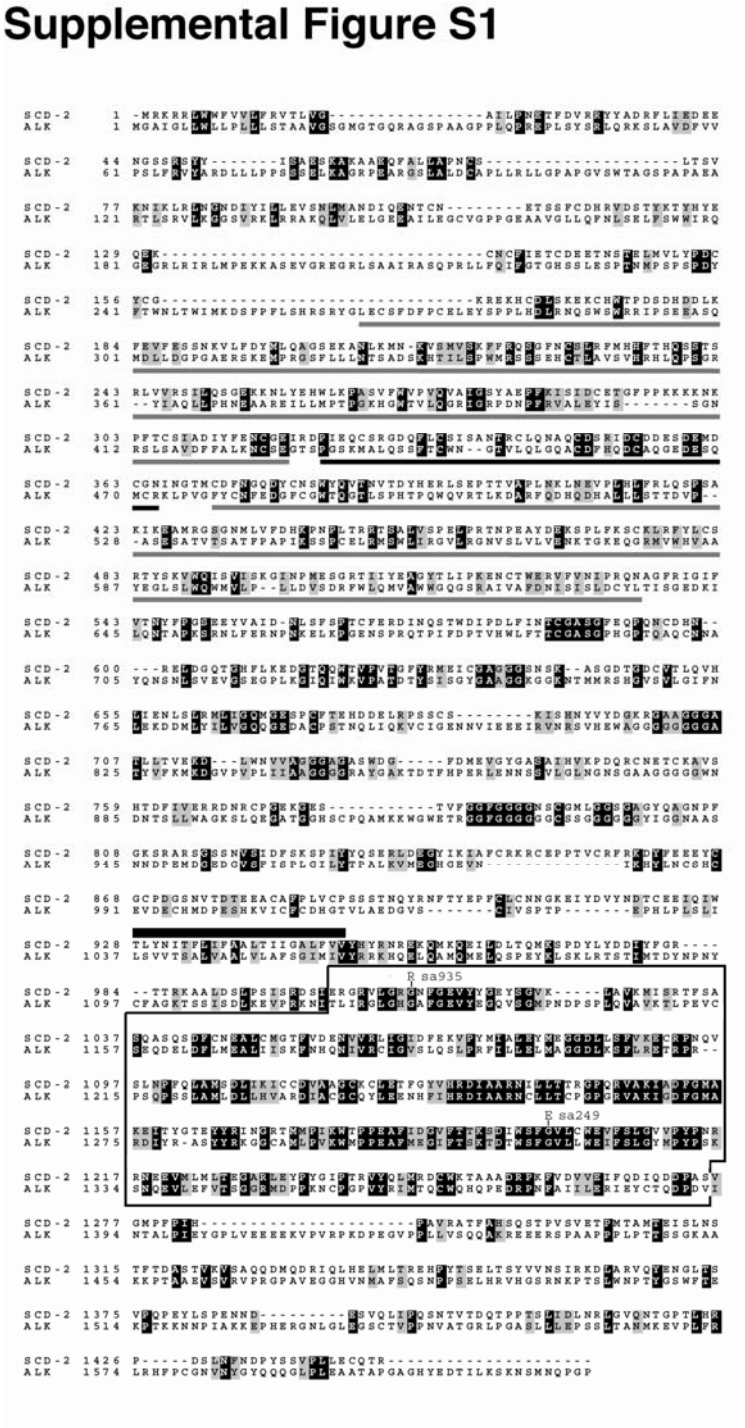

Supplemental Figure S1. A protein sequence alignment of SCD-2 and human ALK. Identical residues are highlighted in black, conserved residues in gray. The MAM domains are underlined with gray, and the LDLRA domain is underlined with black. The putative transmembrane domain has a heavy black bar above it. The kinase domain is boxed, and the amino acid changes of *sa249* and *sa935* are indicated.

Supplemental Figure S2

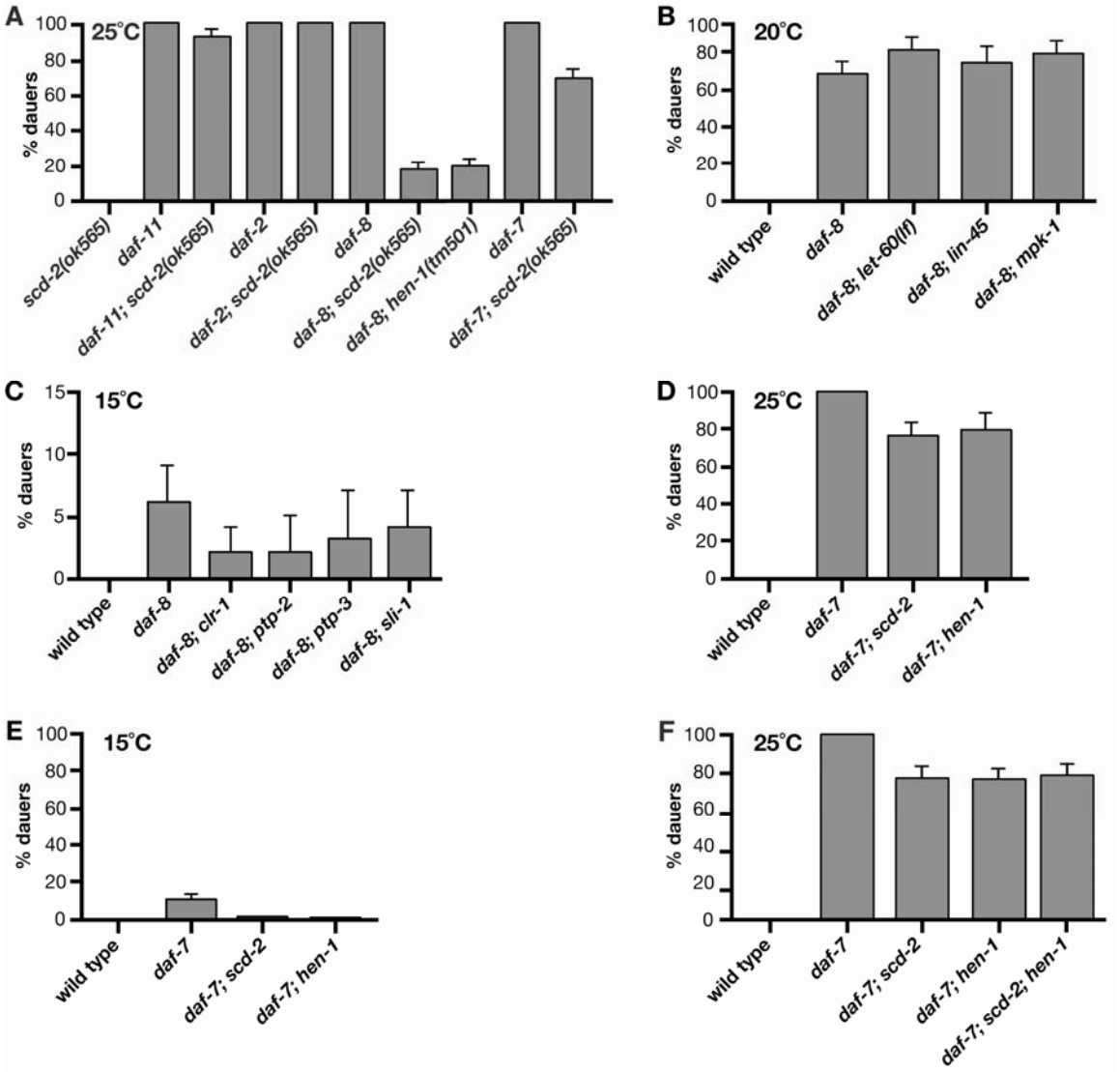

Supplemental Figure S2. Dauer assays of mutants defective in *scd* pathway genes, vulval RTK pathway genes, or negative regulators of RTK signaling. (A) The putative null allele *scd-2(ok565)* displays suppressive phenotypes comparable to *scd-2(sa249)* and *scd-2(y386)*. The *hen-1(tm501)* deletion allele suppresses *daf-8* mutations as successfully as the *scd-2* null allele. (B) Mutations in components of the vulval Ras/MAP Kinase pathway do not suppress *daf-8*. Molecular identities are: LET-60/Ras, LIN-45/Raf, MPK-1/MAP kinase. Not shown are negative results with MEK-2/Mek and SEM-5/Grb2. (C) Known negative regulators of RTK signaling in *C. elegans* do not enhance the *daf-8* Daf-c phenotype at 20°C (not shown) or 15°C (shown). *ptp-2* encodes a non-receptor protein tyrosine phosphatase, *ptp-3* encodes a receptor-like tyrosine phosphatase, *clr-1* encodes a receptor tyrosine phosphatase and *sli-1* encodes a tyrosine kinase negative regulator. (D and E) *scd-2(ok565)* and *hen-1(tm501)* suppress *daf-7(e1372)* at both 25°C and 15°C, indicating that mutation of the *scd-2* pathway does not perturb the temperature sensitivity of dauer formation. (F) The *scd-2(ok565)*; *hen-1(tm501)* double null mutation combination suppresses *daf-7(e1372)* to the same degree as *scd-2* and *hen-1* single mutations. Error bars show the 95% confidence interval calculated based on sample size.

Table S1. The *scd-2* Pathway Regulates TGF-β Transcriptional Output

Genotype	GFP Expression
cuIs5	+++++
cuIs5; scd-2(y386)	+++++
cuIs5; hen-1(tm501)	+++++
cuIs5; sma-5(n678)	+++++
cuIs5; daf-3(e1376)	+++++
daf-2(e1370); *cuIs5*	+++++
cuIs5; *daf-11(m47)*	++++
cuIs5; *daf-11(m47)*; *daf-3(e1376)*	+++++
daf-8(e1393); *cuIs5*	+++
daf-8(e1393); *cuIs5*; *daf-3(e1376)*	+++++
daf-8(e1393); *cuIs5*; *scd-2(sa249)*	++++
daf-8(e1393); *cuIs5*; *scd-2(y386)*	++++
daf-8(e1393); *cuIs5*; *scd-2(ok565)*	++++
daf-8(e1393); *cuIs5*; *sma-5(n678)*	++++
daf-7(e1372); *cuIs5*	+
daf-7(e1372); *cuIs5*; *che-1(p679)*	++

"+" represents barely visible pharyngeal GFP while "+++++" represents wild-type *cuIs5* levels (Figure 5). All experiments (except those involving *hen-1*, *scd-2(ok565)* and *che-1(p679)*) were replicated with the independently isolated *cuIs2* transgene, with the same results. *soc-1* and *che-1* mutations reproducibly restored GFP levels in a *daf-7* (Table 1) but not *daf-8* background (not shown), perhaps because *daf-8* repression of reporter GFP was weak to begin with and *soc-1* and *che-1* suppressor activity is also relatively weak.

Table S2. ASE Regulates Dauer Formation

		% dauers (N)	
Suppressor	Pheromone (N)	*daf-7(e1372)*	*daf-14(m77)*
+	56 (233)	100 (427)	83 (422)
scd-2(ok565)	0 (180)	74 (443)	3 (312)
che-1(p679)	7 (176)	96 (672)	15 (576)
che-1(ot66)	27 (159)	97 (553)	29 (469)
che-1(ot27)	19 (73)	97 (290)	16 (259)
che-1(e1034)	20 (143)	97 (356)	31 (550)

che-1 mutations caused Scd defects weaker than those caused by *scd-2* mutations. This table shows the effect of *scd-2* and *che-1* mutations on the degree of dauer formation at 25˚C in response to pheromone, and in two different Daf-c TGF-β mutant backgrounds, *daf-7(e1372)* and *daf-14(m77)*. "Pheromone" indicates 32 μl exogenous dauer pheromone; "+" indicates no mutation; "N" is the number of animals scored.

Supplemental References

S1. Uchida, O., Nakano, H., Koga, M., and Ohshima, Y. (2003). The *C. elegans che-1* gene encodes a zinc finger transcription factor required for specification of the ASE chemosensory neurons. Development. *130*, 1215-1224.

S2. Chang, S., Johnston, R.J., Jr., and Hobert, O. (2003). A transcriptional regulatory cascade that controls left/right asymmetry in chemosensory neurons of *C. elegans*. Genes Dev. *17*, 2123-2137.

S3. Inoue, T., and Thomas, J.H. (2000). Targets of TGF-beta signaling in *Caenorhabditis elegans* dauer formation. Dev. Biol. *217*, 192-204.

S4. Ishihara, T., Iino, Y., Mohri, A., Mori, I., Gengyo-Ando, K., Mitani, S., and Katsura, I. (2002). HEN-1, a secretory protein with an LDL receptor motif, regulates sensory integration and learning in *Caenorhabditis elegans*. Cell *109*, 639-649.

S5. Brenner, S. (1974). The genetics of Caenorhabditis elegans. Genetics *77*, 71-94.

S6. Horvitz, H.R., Brenner, S., Hodgkin, J., and Herman, R.K. (1979). A uniform genetic nomenclature for the nematode *Caenorhabditis elegans*. Mol. Gen. Genet. *175*, 129-133.

S7. Hodgkin, J., and Doniach, T. (1997). Natural variation and copulatory plug formation in *Caenorhabditis elegans*. Genetics *146*, 149-164.

S8. Inoue, T., and Thomas, J.H. (2000). Suppressors of transforming growth factor-beta pathway mutants in the *Caenorhabditis elegans* dauer formation pathway. Genetics *156*, 1035-1046.

S9. Ailion, M., and Thomas, J.H. (2000). Dauer formation induced by high temperatures in *Caenorhabditis elegans*. Genetics *156*, 1047-1067.

S10. Vowels, J.J., and Thomas, J.H. (1992). Genetic analysis of chemosensory control of dauer formation in *Caenorhabditis elegans*. Genetics *130*, 105-123.

S11. Vowels, J.J., and Thomas, J.H. (1994). Multiple chemosensory defects in *daf-11* and *daf-21* mutants of *Caenorhabditis elegans*. Genetics *138*, 303-316.

S12. Liu, L.X., Spoerke, J.M., Mulligan, E.L., Chen, J., Reardon, B., Westlund, B., Sun, L., Abel, K., Armstrong, B., Hardiman, G., et al. (1999). High-throughput isolation of *Caenorhabditis elegans* deletion mutants. Genome Res. *9*, 859-867.

S13. Huang, L.S., Tzou, P., and Sternberg, P.W. (1994). The *lin-15* locus encodes two negative regulators of *Caenorhabditis elegans* vulval development. Mol. Biol. Cell *5*, 395-411.

S14. Mello, C.C., and Fire, A. (1995). DNA Transformation. In *Caenorhabditis elegans*: Modern Biological Analysis of an Organism, H.F. Epstein and D.C. Shakes, eds. (San Diego: Academic Press), pp. 452-480.